Parametric resonance avoidance of offshore crane cable in subsea lowering operation through A* heuristic planner

Hooi-Siang Kang[1,2], Collin Howe-Hing Tang[1]*, Lee Kee Quen[3], Adelina Steven[4] & Xiaochuan Yu[4]

[1]Faculty of Mechanical Engineering, Universiti Teknologi Malaysia, Johor, Malaysia
[2]Institute for Vehicle System & Engineering (IVeSE), Universiti Teknologi Malaysia, Johor, Malaysia
[3]Malaysia-Japan International Institute of Technology (MJIIT), UTM Kuala Lumpur, Kuala Lumpur, Malaysia
[4]School of Naval Architecture and Marine Engineering, University of New Orleans, New Orleans, Louisiana, USA

*[E-mail: tanghh@utm.my]

Parametric resonance of offshore crane cable was predicted by using Mathieu equation to provide structural safety prediction during subsea lowering operation. This paper studied the predicting method and automatic resonance avoidance of offshore crane cable to complement the safety management during subsea lowering operation. The offshore crane cable was modeled as a tensioned long cylindrical structure and Mathieu instability coefficients were utilized to predict the dynamic instability of the structure. Numerical analyses were conducted to predict the parametric resonance of cable, evaluate the sensitivity of effective submerged length, dynamic tension variation, and plan for resonance avoidance mechanism automatically. Dynamic instability at sub-harmonic 2:1 unstable region of Mathieu stability diagram potentially creates high risk for lowering operation if the damping coefficient is low. Dynamic tension variation can cause instability of offshore crane cable during passing through wave splash zone and landing subsea payload. The reduction of axial tension variation can stabilize the dynamic of offshore crane cable. Parametric resonance of cable is also sensitive to the total payload. The findings of this paper can enhance structural integrity prediction of offshore crane cable and provide an automatic planner to the operator to avoid parametric resonance during subsea lowering operation.

[**Keywords**: parametric resonance; offshore lowering; cable dynamics; Mathieu instability; resonance avoidance; A* heuristic]

Introduction

Lowering subsea structure is an important offshore operation which is commonly conducted during subsea equipment installation, subsea surveillance[1,2], and subsea mining[3]. Offshore crane cable during lowering operation can be assumed as tensioned long cylindrical structure (TLCS) which has physical similarity like mooring lines, top-tensioned risers, and hawsers. Offshore crane cable under loaded condition can be regarded as tensioned structure and it may experience a phenomenon called as parametric resonance. The parametric resonance occurs when a structure is parametrically excited and oscillates at one of its resonant frequencies[4,5]. Parametric excitation differs from forcing since the action appears as a time varying modification on a structural parameter[5]. A small excitation can produce a large response even when the frequency of the excitation is significantly different from the linear natural frequencies of the structure[5,6]. This phenomenon is crucial in assuring the structural health conditions and safety during offshore lowering operation. Hence, an effective prediction on parametric resonance of offshore crane cable is significant for the operator to estimate the allowable working windows for lowering operation and assure the cable structural integrity from disastrous failures.

Parametric resonance of offshore crane cable can be predicted by evaluating the structural dynamic stability. An investigation on the dynamics of TLCS with reduced pretension was reported[7] by focusing on the mooring lines of an

offshore floating structure, named as tensioned-leg platform (TLP). The wave induced time-varying axial tension along the mooring line becomes important in its dynamics when the pretension is reduced and, moreover, the time-varying axial tension variation was found to cause the mooring line to undergo parametric oscillations that can be described by the Mathieu equation[7]. A foundation of mathematical modeling was established[7] to describe the dynamic instability of TLCS in the offshore engineering, which is applicable to describe the parametric resonance of offshore crane cable as well. The complexity of dynamic stability analysis of TLCS was further increased by taking consideration of tension variation[8,9] along the length due to the submerged weight[10] and non-linear dynamic responses[11]. Mathieu's equation was also applied in assessment of parametric response excited by the interactions of vertical excitation forces and lateral dynamics of TLCS[5,12-14]. On the other hand, another mathematical model of parametric resonance, named as Hill's equation, had been studied[15] for multi-frequency excitation source. It can be concluded that Mathieu equation, which is dependent on single-frequency excitation source, can predict more conservative results in the lower vibration modes than the Hill's equation, whereas the multi-frequency excitation is considered[14,15].

From the previous researches, the parametric resonances were mainly assessed for TLCS with top-tensioned conditions[16] and fixed lengths, such as mooring line[13,14], marine riser[15], and suction piles[17]. In this paper, an offshore crane cable was studied to predict the parametric resonance. The main challenges of this study are (i) the effective length of offshore crane cable is continuously changing inside the water domain during lowering subsea structure; and (ii) large dynamic tension variations are occurred during lowering subsea structure through the splash zone and during landing on the targeted location. The objectives of this paper are (i) to model parametric resonance of offshore crane cable based on Mathieu's instability coefficients; (ii) to numerically predict the parametric resonance of offshore crane cable with respect to the variations of effective length, tension variation, and total payload, and (iii) to automatically plan[18,19] submerged effective cable length and dynamic tension variation for parametric resonance avoidance of the offshore crane cable during lowering operation.

Modeling of Parametric Resonance for Offshore Crane Cable

A general damped Mathieu's equation is shown as[20]

$$\ddot{x} + C\dot{x} + (a + b\cos t)x = 0 \qquad (1)$$

where x is the response of vibration, C is damping coefficient, t is time, a and b are the Mathieu's coefficients.

This kind of nonlinear ordinary differential equation (ODE) cannot be solved explicitly[20]. However, by fixing the damping coefficient C, zeros of infinite determinants can be found by specifying a (or b) and searching for the corresponding b (or a) that gives a set of results sufficiently close to zero. The stability of solution of the Mathieu's equation can be graphically represented in the Mathieu stability diagram (MSD)[21]. The parametric resonance of a tensioned cable can be identified by calculating its Mathieu's instability coefficients, and later coordinating the a_n and b_n on a Mathieu's stability diagram (MSD) to obtain a general solution which determines whether the examined structure is in a dynamical stable or unstable region. The Mathieu's coefficients a_n and b_n are with respect to its mode n. The derivation of Mathieu's coefficients of an offshore crane cable under loaded condition is based on the following assumptions: (i) the weight of the offshore crane cable is considered, and it is assumed that the axial tension varies linearly along the water depth[4]; (ii) the direction of the current propagation is assumed to be fixed, and the velocity varies linearly from the bottom to the surface of the sea[4]; (iii) the stiffness and material properties of the offshore crane cable are constant and homogenous along the length of the structure[4]; and (iv) the top-end of crane cable do not move in the horizontal direction[7]. The configuration of single offshore crane cable under loaded condition and force distribution of the corresponding infinitesimal element of cable are described in Fig. 1, where v is the horizontal coordinate, z is vertical coordinate, L is the effective length, $T(t)$ is the cable top tension which is a combined effects of total payload, buoyancy, and crane winch torque, $v(z, t)$ is the lateral motion function, and dz is the length of a finite element. The balance of the horizontal forces in the infinitesimal element can be represented as[4]

$$S_2 - \left(f dz + F_m dz + S_1 \right)$$

$$= S_1 + \frac{\partial S}{\partial z} dz - \left(f dz + F_m dz + S_1 \right)$$

$$= \frac{\partial S}{\partial z} dz - \left(f dz + F_m dz \right)$$

$$= \frac{\partial S}{\partial z} - \left(f + F_m \right) = 0 \tag{2}$$

$$\left[S_1 dz + M_1 \right] - \left[M_2 + T_1 dv \right]$$

$$= \left[S_1 dz + M_1 \right] - \left[M_1 + \frac{\partial M}{\partial z} dz + T_1 dv \right]$$

$$= \left[S_1 dz \right] - \left[\frac{\partial M}{\partial z} dz + T_1 \frac{\partial v}{\partial z} dz \right]$$

$$= \left[S \right] - \left[\frac{\partial M}{\partial z} + T_1 \frac{\partial v}{\partial z} \right] = 0 \tag{3}$$

and the balance of the bending moments in the infinitesimal element is[4]
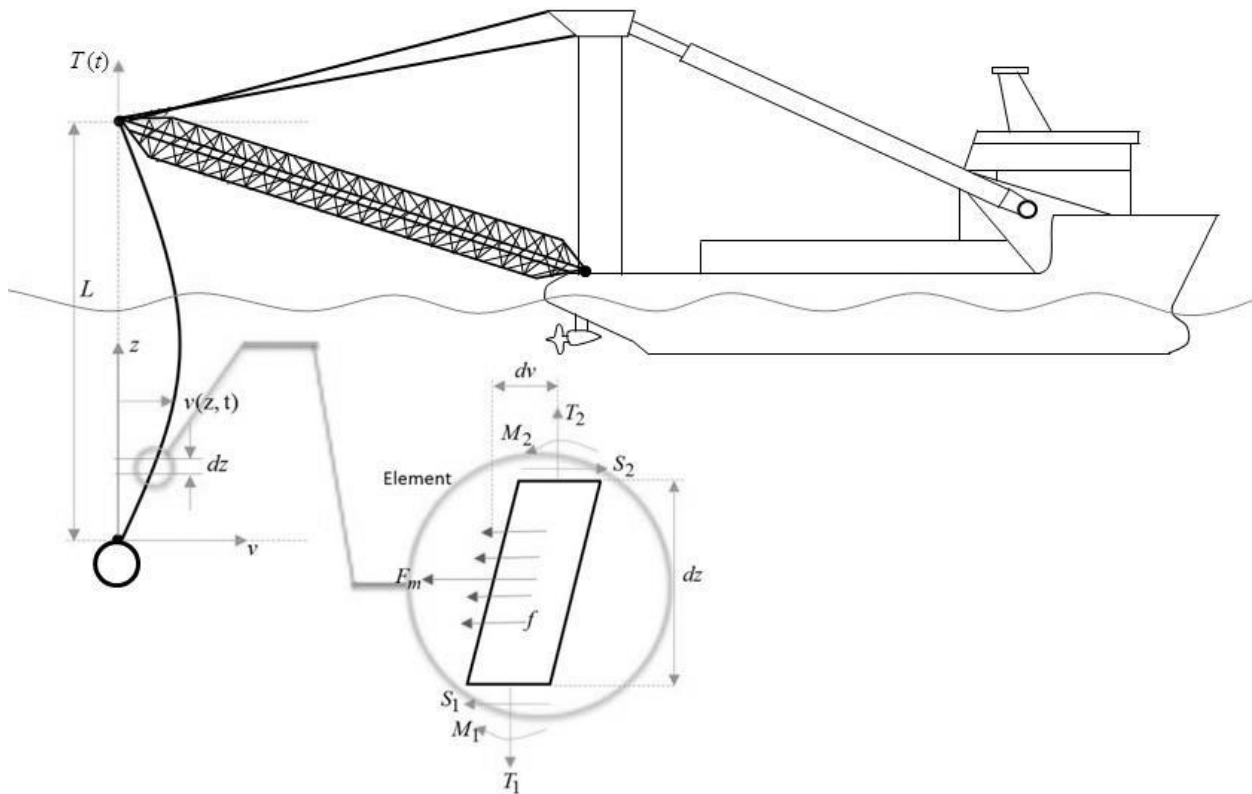

Fig. 1 - Schematic diagram (non-scale) of offshore crane cable with the force distribution of infinitesimal element

where $S_1 = S$ are shear forces, S_2 is shear force equals to $S + (\partial S / \partial z) dz$, $m_l = \pi D h \rho_s + (1/4) \pi D^2 \rho_w + \rho_i A_i$ is mass per unit length, $F_m = m_l \, (\partial^2 v / \partial t^2)$ is inertia force where its direction is opposite to the velocity of lateral motion, D is outer diameter of cable, ρ_s is density of steel, ρ_w is density of seawater. If the cable has hollow cross sectional area, then h is wall thickness, ρ_i is density of internal fluid, and A_i is internal area[4]. C_d is drag coefficient, $f = (1/2) C_d \rho_w D |\partial v / \partial t| (\partial v / \partial t)$ is drag force due to hydrodynamic effect, $M_1 = M = -EI(\partial^2 v / \partial z^2)$ and $M_2 = M + (\partial M / \partial z) dz$ are the bending moments, EI is bending stiffness of cable structure, $T_1 = T =$

$T_0 - (L-z) m_w + \Delta T \delta(t)$ and $T_2 = T + (\partial T / \partial z) dz$ are tensions in the cable, $\partial T / \partial z = m_w$ is cable wet weight per unit length, $dv = (\partial T / \partial z) \, dz$ is the difference between the displacements of the upper and lower points of the infinitesimal element dz[4].

By substituting (3) into (2), the coupling equation of the force and moment are defined as

$$\frac{\partial S}{\partial z} = \left(f + F_m \right) \tag{4}$$

$$\frac{\partial}{\partial z} \left(\frac{\partial M}{\partial z} + T \frac{\partial v}{\partial z} \right) = \frac{1}{2} C_d \rho_w D \left| \frac{\partial v}{\partial t} \right| \frac{\partial v}{\partial t} + m_l \frac{\partial^2 v}{\partial t^2} \tag{5}$$

$$m_l \frac{\partial^2 v}{\partial t^2} + \frac{1}{2} C_d \rho_w D \left| \frac{\partial v}{\partial t} \right| \frac{\partial v}{\partial t}$$
$$+ \frac{\partial^2}{\partial z^2} \left(EI \frac{\partial^2 v}{\partial z^2} \right) - \frac{\partial}{\partial z} \left(T \frac{\partial v}{\partial z} \right) = 0 \tag{6}$$

and (6) can be further rearranged as

$$m_l \frac{\partial^2 v}{\partial t^2} + \frac{1}{2} C_d \rho_w D \left| \frac{\partial v}{\partial t} \right| \frac{\partial v}{\partial t} + EI \frac{\partial^4 v}{\partial z^4}$$
$$- \frac{\partial}{\partial z} \left(\begin{bmatrix} T_0 - (L-z) m_w \\ + \Delta T \delta(t) \end{bmatrix} \frac{\partial v}{\partial z} \right) = 0 \tag{7}$$

$$m_l \frac{\partial^2 v}{\partial t^2} + \frac{1}{2} C_d \rho_w D \left| \frac{\partial v}{\partial t} \right| \frac{\partial v}{\partial t}$$
$$+ EI \frac{\partial^4 v}{\partial z^4} - T \frac{\partial^2 v}{\partial z^2} - m_w \frac{\partial v}{\partial z} = 0 \tag{8}$$

where $\delta(t)$ is variation of axial tension. The time varying axial tension causes the offshore crane cable to undergo parametric oscillations. However, even if it is in an unstable condition, the quadratic fluid damping force limits the amplitude of the lateral motion[7]. The variation of axial tension is modeled by the following irregular process[7]

$$\delta(t) = \sum_{n=0}^{\infty} a_n \cos(\omega_n t + \varepsilon_n) \tag{9}$$

where ω_n is the natural frequency of the lateral vibration of the cable, ε_n is the phase angle. The wave induced axial tension is assumed to be sinusoidal. This assumption is based on the fact that even if ocean waves are irregular, the time-varying axial tension become more regular (that is a narrower banded spectrum) due to the transfer function from wave action to tensioned cylindrical structure forces[7]. Despite irregular incident waves, the inertia of host vessel can cause the resultant cable axial tension to tend towards near sinusoidal oscillations. The offshore crane cable tension in (8) can therefore be defined as[7]

$$T = T_0 - (L-z) m_w + \Delta T \delta(t)$$
$$= T_0 - (L-z) m_w + \Delta T \sum_{n=0}^{\infty} a_n \cos(\omega_n t + \varepsilon_n) \tag{10}$$

where T_0 is pretension of the cable at the crane tip, and ΔT is the amplitude of tension variation.

Taking the fundamental mode (the largest amplitude mode of the model) only and using the method of separation of variables[7,22], the expansion of each linear vibration mode is

$$v(z,t) = \sum_m \phi_m(t) u_m(z) \tag{11}$$

where ϕ_m is the temporal variable and u_m is the spatial variable. By substituting (11) into (8), the coupling equation of the force and moment in an infinitesimal element of offshore crane cable can be represented as

$$m_l \frac{\partial^2 \sum_m \phi_m(t) u_m(z)}{\partial t^2} +$$
$$\left(\frac{1}{2} C_d \rho_w D \left| \frac{\partial \sum_m \phi_m(t) u_m(z)}{\partial t} \right| \frac{\partial \sum_m \phi_m(t) u_m(z)}{\partial t} \right)$$
$$+ EI \frac{\partial^4 \sum_m \phi_m(t) u_m(z)}{\partial z^4} - T \frac{\partial^2 \sum_m \phi_m(t) u_m(z)}{\partial z^2}$$
$$- m_w \frac{\partial \sum_m \phi_m(t) u_m(z)}{\partial z} = 0 \tag{12}$$

Equation (12) can be rewritten into a compact form as

$$\sum_m \begin{cases} m_l \phi_m''(t) u_m(z) + \\ \left(\begin{matrix} \frac{1}{2} C_d \rho_w D \times \\ \left| \phi_m'(t) u_m(z) \right| \phi_m'(t) u_m(z) \end{matrix} \right) \\ + EI \phi_m(t) u_m^{(4)}(z) \\ - T \phi_m(t) u_m''(z) - m_w \phi_m(t) u_m'(z) \end{cases} = 0 \tag{13}$$

Considering that the boundary conditions of both ends of cable are assumed to be pinned-pinned connection, the special function of spatial variable that satisfies the boundary conditions is[4]

$$u_m(z) = \sin\left(\frac{n\pi}{L} z \right) \tag{14}$$

Because of u_m is mutually orthogonal when its mode m varies, by applying Galerkin's method on (13)[23], the coupling equation of the force and moment in an infinitesimal element of tensioned cable are defined as

$$\int_0^L \sum_m \left\{ \begin{array}{l} m_l \phi_m''(t) u_m(z) + \dfrac{1}{2} C_d \rho_w D \\ \times \left| \phi_m'(t) u_m(z) \right| \phi_m'(t) u_m(z) \\ + EI \phi_m(t) u_m^{(4)}(z) \\ - T \phi_m(t) u_m''(z) \\ - m_w \phi_m(t) u_m'(z) \end{array} \right\} \cdot u_n dz = 0 \tag{15}$$

The solution of (15) is the coupling equation of the force and moment in an infinitesimal element of offshore crane cable, which can be represented as

$$m_l \int_0^L u_n^2 dz \phi_n''(t)$$
$$+ \frac{1}{2} C_d \rho_w D \int_0^L |u_n| u_n^2 dz \left| \phi_n'(t) \right| \phi_n'(t)$$
$$+ \left(\begin{array}{l} EI \int_0^L u_n^{(4)} \cdot u_n dz - \int_0^L T u_n'' \cdot u_n dz \\ - m_w \int_0^L u_n' \cdot u_n dz \end{array} \right) \phi_n(t) = 0 \tag{16}$$

Equation (16) can be further rearranged into the form of Mathieu equation as shown in (1), and it is convenient to introduce a dimensionless time variable $\tau = \omega t$ into the coupling equation[4]

$$\phi_n''(\tau) +$$
$$\frac{\frac{1}{2} C_d \rho_w D \int_0^L |u_n| u_n^2 dz}{m_l \int_0^L u_n^2 dz \cdot \omega} \left| \phi_n'(\tau) \right| \phi_n'(\tau) +$$
$$\frac{\left(\begin{array}{l} EI \int_0^L u_n^{(4)} \cdot u_n dz - \int_0^L T u_n'' \cdot u_n dz \\ - m_w \int_0^L u_n' \cdot u_n dz \end{array} \right)}{m_l \int_0^L u_n^2 dz \cdot \omega^2} \phi_n(\tau) = 0 \tag{17}$$

Equation (17) can be rewritten in the following form in order to determine the Mathieu's coefficients a_n, b_n, C,

$$\phi_n''(\tau) + C \phi_n'(\tau) +$$
$$\left[a_n + b_n \sum_{n=0}^\infty a_n \cos\left(\frac{\omega_n}{\omega} \tau + \varepsilon_n \right) \right] \phi_n(\tau) = 0 \tag{18}$$

where $n = 1,2,3\ldots$, therefore, the nonlinear damping coefficient C in (18) can be derived as[7]

$$C = \frac{\frac{1}{2} C_d \rho_w D \int_0^L |u_n| u_n^2 dz}{m_l \int_0^L u_n^2 dz \cdot \omega} \cdot \left| \phi_n'(\tau) \right|$$
$$= \frac{C_d \rho_w D}{2 m_l \omega} \cdot \frac{8}{3\pi} \cdot \left| \phi_n'(\tau) \right| = \frac{4 C_d \rho_w D}{3\pi m_l \omega} \cdot \left| \phi_n'(\tau) \right| \tag{19}$$

The damping coefficient C is dependent of the maximum velocity[14] of the cable in transverse motion V_{max}. Hence, (19) can be further simplified as

$$C = \frac{4 C_d \rho_w D}{3\pi m_l \omega} \cdot \left| \phi_n'(\tau) \right| = \frac{4 C_d \rho_w D V_{max}}{3\pi m_l \omega} \tag{20}$$

Also, the stiffness terms in (17) can be further derived as

$$\frac{EI \int_0^L u_n^{(4)} \cdot u_n dz}{m_l \int_0^L u_n^2 dz \cdot \omega^2}$$
$$- \frac{\int_0^L T u_n'' \cdot u_n dz}{m_l \int_0^L u_n^2 dz \cdot \omega^2} - \frac{m_w \int_0^L u_n' \cdot u_n dz}{m_l \int_0^L u_n^2 dz \cdot \omega^2} \tag{21}$$

By using the special function in (14), the stiffness terms in (21) can be rewritten as

$$\frac{EI \left(\frac{n\pi}{L} \right)^4 + T_0 \left(\frac{n\pi}{L} \right)^2 - \frac{1}{2} m_w L \left(\frac{n\pi}{L} \right)^2}{m_l \omega^2}$$
$$+ \frac{\Delta T \left(\frac{n\pi}{L} \right)^2 \sum_{n=0}^\infty a_n \cos\left(\omega_n t + \varepsilon_n \right)}{m_l \omega^2} \tag{22}$$

By compared to (18), the Mathieu's coefficient a_n is defined as[24]

$$a_n = \frac{\left(EI \left(\frac{n\pi}{L} \right)^4 + T_0 \left(\frac{n\pi}{L} \right)^2 - \frac{1}{2} m_w L \left(\frac{n\pi}{L} \right)^2 \right)}{m_l \omega^2}$$
$$= \frac{\omega_n^2}{\omega^2} = \left(\frac{\omega_n}{\omega} \right)^2 \tag{23}$$

where ω is the basic frequency of the external excitation on the transverse direction of the

offshore crane cable, and

$$\omega_n = \left(\frac{n\pi}{L}\right)\sqrt{\frac{EI\left(\frac{n\pi}{L}\right)^2 + T_0 - \frac{1}{2}m_w L}{m_l}} \qquad (24)$$

Also, the Mathieu's coefficient b_n is defined as[24]

$$b_n = \frac{\Delta T\left(\frac{n\pi}{L}\right)^2}{m_l \omega^2} \qquad (25)$$

Modeling of Automatic Parametric Resonance Avoidance Planner

Based on the Mathieu stability diagram with respect to different critical damping ratio values as shown in Fig. 2, useful information regarding optimal offshore crane cable lowering processes, especially effective length L and tension variation ΔT can be extracted. Automatic planning has been receiving more interests in the modern offshore operations[25-28]. By incorporating A* heuristic machine planning algorithm into the whole decision making and offshore crane cable lowering process control, the dynamic stability of subsea structure lowering operations can be improved. However, as the two dimensions depicted by Mathieu stability criterion are mainly related to a_n and b_n, these two coefficients could not be readily applied in the process control of offshore crane cable lowering operation. Therefore, a configuration space with L-ΔT dimensions, which is more user-friendly to machine control operation, has to be constructed with reference to the Mathieu stability coefficients a_n and b_n. The range of configuration space was pre-determined in such a way that effective submerged length L of cable was in the range from 100 m below mean water level (MWL) to 500 m below MWL, and dynamic axial tension variation of cable ΔT was varying from 10 kN to 100 kN. The mapping between configuration space and Mathieu stability coefficients was achieved through (23) and (25). With the constructed L-ΔT configuration space, the offshore crane cable lowering processes can now be significantly optimized through the use of A* heuristic planner to search for a series of most optimum L and ΔT, whilst at the same time trying to avoid the instable regions in Mathieu stability diagram.
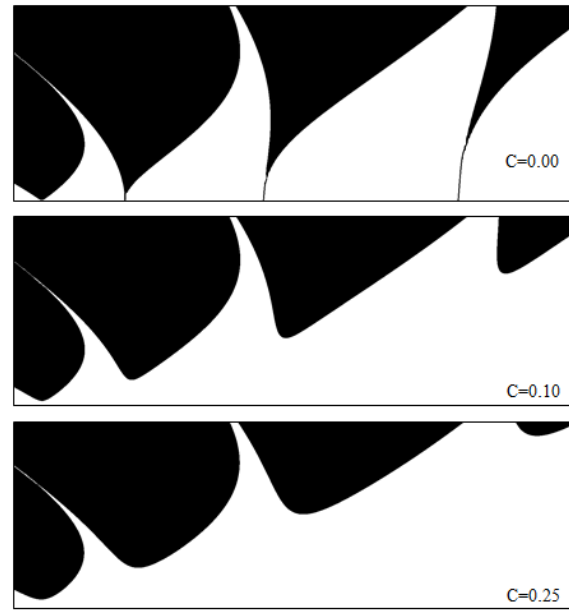

Fig. 2 - Mathieu stability diagram for automatic effective cable length and tension variation prediction.

An automatic planning for parametric resonance avoidance by this approach can avoid the risk of driving the crane cable into the instable regions which induces parametric resonance as predicted. The search for most optimum series of L and ΔT is indeed a typical path planning problem. Knowing that the initial and targeted operating points are N_S and N_G respectively, the A* heuristic planner will determine the most optimum series of L and ΔT based on the cost function $f(N_{i+1})$ given as follows[29]

$$\begin{cases} f(N_{i+1}) = g(N_{i+1}) + h(N_{i+1}) \\ g(N_{i+1}) = g(N_i) + c(N_i, N_{i+1}) \end{cases} \qquad (26)$$

In (26), $c(N_i, N_{i+1})$ is the cost of action moving from point N_i to N_{i+1}. In this paper, the heuristic function $h(N_{i+1})$ is estimated from the distance between the successor point N_{i+1} and the targeted point N_G. The estimation of $h(N_{i+1})$ is given as follows

$$h(N_{i+1}) = \sqrt{\left(L_{N_{i+1}} - L_{N_G}\right)^2 + \left(\Delta T_{N_{i+1}} - \Delta T_{N_G}\right)^2} \qquad (27)$$

Numerical Simulation of Parametric Resonance and Resonance Avoidance for Offshore Crane Cable

In this section, the prediction of parametric resonance for an offshore crane cable under loaded condition was simulated. The first

vibration mode which has largest amplitude[14] was predicted by using the Mathieu stability diagram. This prediction can calculate more conservative results in the lower modes than the Hill's equation[15]. The configuration of offshore crane cable is listed in Table 1. Later, the parametric resonance avoidance was conducted by using A* heuristic automatic planning based on the cases matrix as tabulated in Table 2.

Table 1 - Configuration of offshore crane cable

Operational water depth	100 m - 500 m
Top pretension (T_0)	5.0 MT
Cable diameter	0.05 m
Cable maximum length	500 m
Wet weight per unit length (m_w)	0.01342 MT/m
Mass per unit length (m_l)	15.43 kg/m
Bending stiffness (EI)	6.48 MT.m^2
Excitation frequency (ω)	1.0472 rad/s
Density of sea water (ρ_w)	1.025 MT/m^3
Density of steel (ρ_s)	7.86 T/m^3

Results and Discussion

A main challenge to predict the parametric resonance of offshore crane cable is during the stage of lowering subsea structure passing through the water column in vertical direction. The effective length of cable is continuously changing inside water domain. The axial tension variation of the cable is relatively consistent in this stage and which is mainly caused by vessel motion[30]. In this prediction, the dynamic tension variation in this stage is assumed as 40 kN. The Mathieu instability assessment of offshore crane cable with respect to the variation of effective length is shown in Fig. 3.

As the effective length of offshore crane cable increasing from 100 m to 500 m submerged depth in the water column, the first mode of cable motion is going to transform across three instability regions as illustrated in Fig. 3. When the effective lengths are in between 110 m to 120 m, the parametric resonance in lateral direction is predicted when the operational point (combined coordinates of a_n and b_n) passing through the unstable 1:2 region. However, the range of dynamic instability is only lasting for few meters at this region. The second parametric resonance is predicted when further lowering the cable to its effective length from 170 m to 190 m.

Table 2 - Case matrix for automatic cable length and tension variations planning

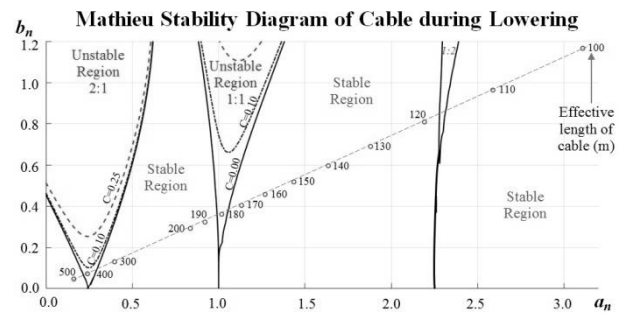| Case	Critical damping ratio	Maximum allowable tension variation, ΔT (kN)	Operational water depth for automatic planning
Undamped	0.00	15	
		30	
		45	
Lightly damped	0.10	15	110 m – 450 m
		30	
		45	
		75	
Highly damped	0.25	15	
		30	
		45	
		90	

Fig. 3 - Mathieu instability assessment of offshore crane cable with variation of effective length.

The cable is in parametric resonance when this effective length is 180 m, which is inside the unstable 1:1 region. The range of dynamic instability in this 1:1 region is longer than the 1:2 region. As lowering of subsea structure to 400 m submerged depth, the cable parametric resonance is predicted at the 2:1 sub-harmonic region. It is noteworthy that the range of dynamic instability in this 2:1 region is lasting for almost one hundred meters and, therefore, it can cause high risk lowering operation to the operator. For longer cable length in deep water, very small values of the parameters a_n and b_n are potential to induce the lateral vibration of cable. As the cable's effective length increases during lowering subsea structure, the operating point in the Mathieu stability diagram tends to the region near its origin (where the a_n and b_n are smaller). The dynamic behavior is very sensitive to small variations in the parameters a_n and b_n in the sub-harmonic 2:1 region.

The damping coefficient C is dependent on the maximum velocity V_{max} of the cable in the transverse motion[14]. The parameters that can be controlled from the design stage to adjust the nonlinear damping coefficient C of the cable are drag coefficient C_d, cable diameter D, and mass per unit length m_l, as stated in (20)[15]. The nonlinear damping coefficient C for the cable in this case is $C = 1.346C_d \times V_{max}$, where it is highly influenced by the drag coefficient C_d and maximum lateral velocity V_{max} of the cable. This information is useful for the operator to determine the windows of subsea lowering operation and to design action plan for rectifying the dynamic instability of cable. For instance, the parametric resonance of cable in the sub-harmonic unstable 2:1 region can be significantly suppressed by increasing the lateral damping. If the drag coefficient C_d is 0.7 in this case, a velocity V_{max} more than 0.106 m/s can increase the damping coefficient C to 0.10 of critical damping. This control can be reasonably achieved by dynamic positioning of the service vessel.

The subsea lowering operation can be divided into different stages, and sensitive parameters are different at each stage. Large dynamic tension variation is occurred during (i) lowering subsea structure through the splash zone, and during (ii) landing payload on the targeted location. The Mathieu instability assessment of offshore crane cable with respect to the variations of axial tension is shown in Fig. 4.

During passing through the splash zone, submerged volume and hydrodynamic parameters vary throughout a wave period and, moreover, the combination of direct wave load and load due to vessel motion may cause peak dynamic tension variation[30]. Also, during landing payload on the targeted location, a peak dynamic tension variation may occur if the subsea structure is further lifted from the initial landed point due to crane uplift motion before the lifting cable is slack[30]. To predict the parametric resonance during these two stages, the Mathieu instability of offshore crane cable is examined with respect to the dynamic tension variation. It is reasonable to assume that the changes of effective cable length during these two operational stages are relatively small and, hence, constant lengths are given to simulate the parametric resonance for both stages, which are 170 m submerged depth for splash zone and 500 m for landing payload, respectively.
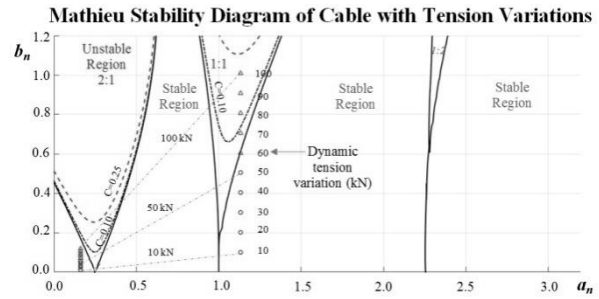

Fig. 4 - Mathieu stability assessment of offshore crane cable with variation of axial tension.

From the first mode as illustrated in Fig. 4, if the axial tension variation ΔT is larger, the operating point shifts towards the unstable region. The reduction of axial tension variation ΔT can move the operating point towards a stable region. This finding provides a meaningful control method by using force control to maintain the stability of offshore crane cable even if the available lateral damping is low. The sensitivity of tension variation is larger in the 1:1 unstable region compared to sub-harmonic 2:1 unstable region. In this simulation, the parametric resonance in splash zone can be avoided as long as the dynamic tension variation of cable is maintained below 60 kN. Since the payload dry weight in this case is five metric tons, an allowable dynamic tension variation of 60 kN can be defined as a large working window for the subsea installation operator.

Another useful prediction for subsea lowering installation is to assess the sensitivity of cable's parametric resonance with respect to the variation of pretension, which is determined by the total payload in force equilibrium state. The Mathieu instability assessment of offshore crane cable with respect to the variation of pretension is shown in Fig. 5.

For the case of three metric tons pretension, the operating point shifts towards sub-harmonic 2:1 unstable region if the pretension of the cable is reduced. On the other hand, if the pretension of cable is increased, the operating point shifts towards the 1:1 unstable region. It is noteworthy that a slight damping coefficient ($C = 0.10$ of critical damping, for instance) on the 1:1 unstable region can transform the unstable condition to a stable condition. However, the sub-harmonic 2:1 unstable region is relatively less influenced by the damping coefficient compared to the 1:1 unstable region, a very large damping coefficient is required to rectify the cable instability in the sub-harmonic 2:1 unstable region.
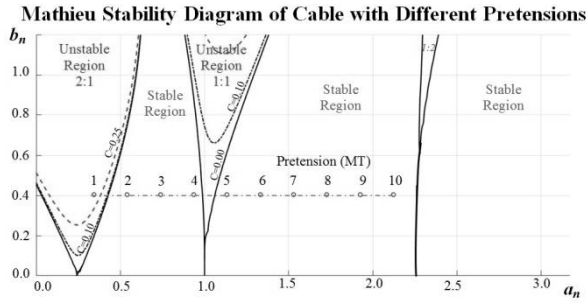
Fig. 5 - Mathieu stability assessment of offshore crane cable with variation of pretension.

The parametric resonance avoidance for offshore crane cable lowering length and its axial dynamic tension variations was automatically planned by A* heuristic algorithm in *L-ΔT* configuration space, as shown in Fig. 6(a). Three maximum allowable axial dynamic tension variations were tested for lowering a crane cable from 110 m below MWL to 450 m below MWL. It can be found that, in accordance with the results in Fig. 3, the larger dynamic tension variation has bigger tendency to cause the cable's instability. The initial position of crane cable was at 110 m below MWL and it was simulated to be lowered down to the targeted water depth at 450 m below MWL. If the dynamic tension variation was maintained at 15 kN, the overall lowering process was conducted within stable region even though under the undamped condition. However, if the initial dynamic tension variation was started at 35 kN or 45 kN in this case, the automatic planning for parametric resonance avoidance reduced the allowable operating dynamic tension variation of cable to 25 kN when the submerged cable at around 170 m below MWL to avoid the predicted Mathieu instability of cable to be induced in the 1:1 unstable region. The maximum allowable dynamic tension variation will be maintained at 25 kN until the cable was lowered to 350 m below MWL, where after the submerged cable passing sub-harmonic 2:1 unstable region.

The offshore lowering process in MSD diagram is shown in Fig. 6(b) where it can be found that the coordinates of a_n and b_n were always located in the stable region.

The effect of lateral damping was introduced in the damped cases, where the results of critical damping ratio $c = 0.10$ and $c = 0.25$ are shown in Fig. 7(a-b) and Fig. 8(a-b) respectively. Since the

existence of damping can improve the parametric stability of cable, larger maximum dynamic tension variation can be tested in these lightly damped ($c = 0.10$) and highly damped ($c = 0.25$) cases. As illustrated in Fig. 7(a) and Fig. 8(a), the parametric resonance avoidance in *L-ΔT* space was significant when the maximum allowable tension variations *ΔT* are increased. As shown in the lightly damped case in Fig. 7(a), if the dynamic tension variation was started at 75 kN, the allowable dynamic tension variation was automatically reduced to nearly 65 kN when the submerged cable length was at 170 m below MWL to avoid the cable instability as predicted in the 1:1 unstable region.
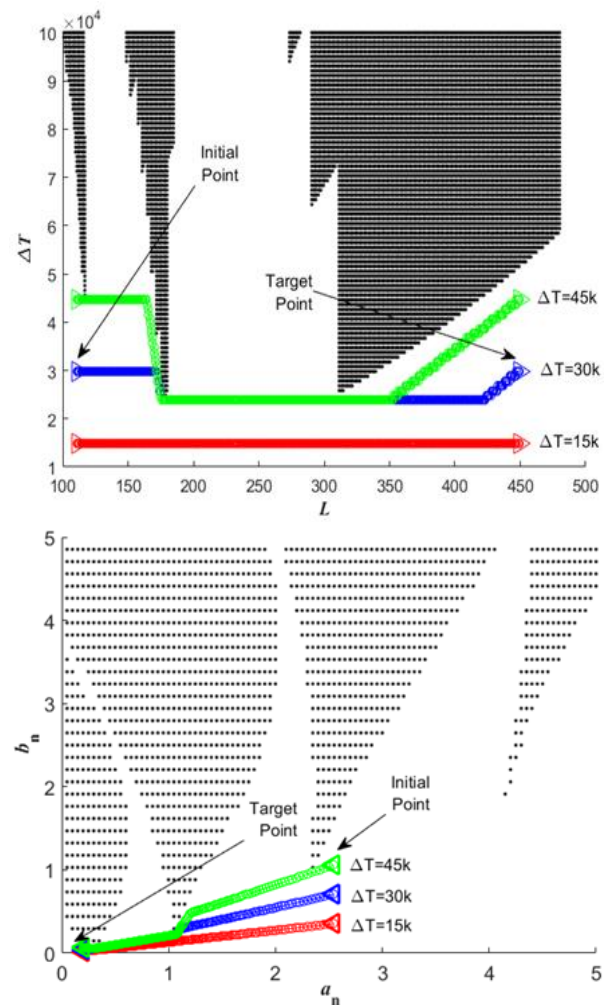

Fig. 6 - Automatic cable length and tension variation planning for parametric resonance avoidance in undamped case, (a) in *L-ΔT* space, and (b) in MSD.
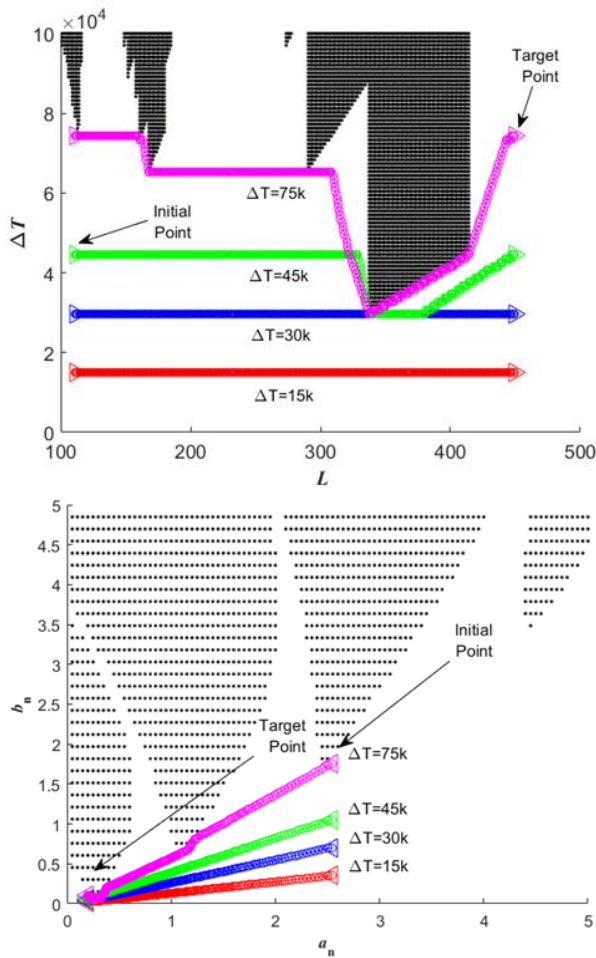
Fig. 7 - Automatic cable length and tension variation planning for parametric resonance avoidance when damping coefficient is 0.10 of critical damping, (a) in L-ΔT space, and (b) in MSD.
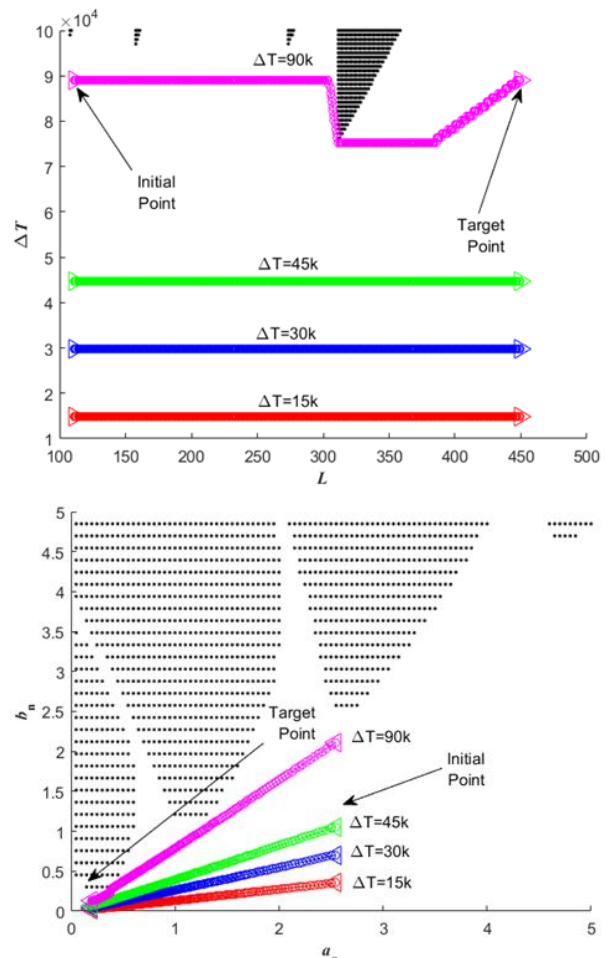

Fig. 8 - Automatic cable length and tension variation planning for parametric resonance avoidance when damping coefficient is 0.25 of critical damping, (a) in L-ΔT space, and (b) in MSD.

The allowable dynamic tension variation was further gradually reduced to 30 kN when the submerged cable length was at 310 m below MWL to avoid the parametric resonance of submerged cable when it passing sub-harmonic 2:1 unstable region.

In the case of highly damped, the total stable zone is larger. Hence, maximum allowable dynamic tension variation can be further enlarged. It can be found that the low-side tested maximum allowable tension variations (45 kN, 30 kN, and 15 kN) were kept unchanged throughout the crane cable lowering operation. On the other hand, only high tension variation, such as 90 kN was reduced by automatic parametric resonance avoidance planning. The offshore lowering process in MSD diagrams for damped cases are shown in Fig. 7(b) and Fig. 8(b), where it can be found that the coordinates of a_n and b_n were always located in the stable region.

Conclusions

Dynamic stability of offshore crane cable is significant to assure cable's structural integrity during subsea lowering operation. Parametric resonance can be adequately predicted by using Mathieu equation which provides relatively conservative results. From the study in this paper, it can be concluded that:

- Lowering offshore crane cable in deep water can induce parametric resonance for more than one hundred meters of vertical lowering range before it has exceeded from the sub-harmonic 2:1 unstable region if the nonlinear damping coefficient is low.
- The influence of dynamic tension variation to the parametric resonance of offshore crane cable during passing through wave splash zone and landing subsea payload are relatively smaller.
- Variation of service payload can cause either stability or instability. Sensitivity of

payload to parametric resonance is highly recommended to be assessed before every lowering operation.

- Automatic parametric resonance avoidance was developed in A* heuristic algorithm to control the submerged cable length and dynamic axial tension variations to avoid the dynamic instability of crane cable during offshore lowering operation.

Acknowledgements

References

1. Xiang, X., Yu, C., and Zhang, Q., On intelligent risk analysis and critical decision of underwater robotic vehicles, *Ocean Engineering*, 140(2017) 453-465.

2. Xiang, X., Yu, C., and Zhang, Q., Robust fuzzy 3D path following for autonomous underwater vehicle subject to uncertainties, *Computers & Operations Research*, 84(2017) 165-177.

3. Kang, H.S., Wu, Y.T., Lee, K.Q., Tang, C.H.H., and Siow, C.L., Underwater target tracking of offshore crane system in subsea operations, in: *Modeling, design and simulation of systems*, edited by Mohamed Ali, M., Wahid, H., Mohd Subha, N., Sahlan, S., Md. Yunus, M., Wahap, A., (Springer Nature, Singapore) 2017, pp. 126-137.

4. Xiao, F., and Yang, H.Z., Probabilistic assessment of parametric instability of a top tensioned riser in irregular waves, *Marine Science and Technology*, 19(2014) 245-256.

5. Radhakrishnan, S., Datla, R., and Hires, R.I., Theoretical and experimental analysis of tethered buoy instability in gravity waves, *Ocean Engineering*, 34(2007) 261-274.

6. Nayfeh, A.H., and Balachandran, B., *Applied nonlinear dynamics: analytical, computational and experimental methods*, (Wiley, New Jersey) 2008, pp. 277-421.

7. Patel, M.H., and Park, H.I., Dynamics of tension leg platform tethers at low tension. Part I - Mathieu stability at large parameters, *Marine Structures*, 4(1991) 257-273.

8. Kang, H.S., Kim, M.H., Bhat Aramanadka, S.S., Kang, H.Y., Lee, K.Q., Suppression of tension variations in hydro-pneumatic riser tensioner by using force compensation control, *Ocean Systems Engineering*, 7(2017) 225-246.

9. Kang, H.S., Kim, M.H., Bhat Aramanadka, S.S., Tension variations of hydro-pneumatic riser tensioner and implications for dry-tree interface in semisubmersible, *Ocean Systems Engineering*, 7(2017) 21-38.

10. Simos, A.N., and Pesce, C.P., Mathieu stability in the dynamics of TLP's tethers considering variable tension along the length, *Transactions on the Built Environment*, 29(1997) 175-186.

11. Chatjigeorgiou, I.K., and Mavrakos, S.A., Bounded and unbounded coupled transverse response of parametrically excited vertical marine risers and tensioned cable legs for marine applications, *Applied Ocean Research*, 24(2002) 341-354.

12. Zhang, L.B., Zou, J., and Huang, E.W., Mathieu instability evaluation for DDCV/Spar and TLP tendon design, paper presented at the *11th Offshore Symposium*, Houston, USA, 2002.

13. Chandrasekaran, S., Chandak, N.R., and Anupam, G., Stability analysis of TLP tethers, *Ocean Engineering*, 33(2006) 471-482.

14. Wang, T., and Zou, J., Hydrodynamics in deepwater TLP tendon design, *Hydrodynamics, Ser. B*, 18(2006) 386-393.

15. Yang, H., Xiao, F., and Xu, P., Parametric instability prediction in a top-tensioned riser in irregular waves, *Ocean Engineering*, 70(2013) 39-50.

16. Kang, H.S., Kim, M.H., Aramanadka, S.S.B., and Kang, H.Y., Dynamic response control of top-tension risers by a variable damping and stiffness system with magneto-rheological damper, paper presented at the *33rd Int. Conf. on Ocean, Offshore and Arctic Engineering (OMAE2014)*, San Francisco, California, USA, 2014.

17. Huang, L., Zhang, J., Yu, X., Randall, R.E., and Wilde, B., Numerical simulation on dynamics of suction piles during lowering operations, paper presented at the *21st Int. Offshore and Polar Eng. Conf.*, Hawaii, USA, 2011.

18. Xiang, X., Yu, C., and Zhang, Q., Robust fuzzy 3D path following for autonomous underwater vehicle subject to uncertainties, *Computers & Operations Research*, 84(2017) 165-177.

19. Xiang, X., Yu, C., Niu, Z., Zhang, Q., Subsea cable tracking by autonomous underwater vehicle with magnetic sensing guidance, *Sensors*, 16(2016) 1335.

20. Koo, B.J., Kim, M.H., and Randall, R.E., Mathieu instability of a Spar platform with mooring and risers, *Ocean Engineering*, 31(2004) 2175-2208.

21. Moideen, H., *Prediction of parametric roll of ships in regular and irregular sea*, Master thesis, Texas A&M University, USA, 2010.

22. Nayfeh, A.H., and Mook, D.T., Parametric excitations of linear systems having many degrees of freedom, *Acoustical Society of America*, 62(1977) 375-381.

23. Brugmans, J., *Parametric instability of deep-water risers*, Master thesis, Delft University of Technology, the Netherlands, 2005.

24. Yang, H., and Xiao, F., Instability analyses of a top-tensioned riser under combined vortex and multi-frequency parametric excitations, *Ocean Engineering*, 81(2014) 12-28.

25. Xiang, X., Yu, C., Lapierre, L., Zhang, J., and Zhang, Q., Survey on fuzzy-logic-based guidance and control of marine surface vehicles and underwater vehicles, *International Journal of Fuzzy Systems*, 3(2017) 1-15.

26. Xiang, X., Liu, C., Su, H., and Zhang, Q., On decentralized adaptive full-order sliding mode control of multiple UAVs. *ISA Transactions*, (2017) (in press)

27. Khalid, I., Arshad, M.R., and Ishak, S., A hybrid-driven underwater glider model, hydrodynamics estimation, and an analysis of the motion control, *Ocean Engineering*, 81(2014) 111–129.

28. Xiang, X., Lapierre, L., and Jouvencel, B., Smooth transition of AUV motion control: From fully-actuated to under-actuated configuration, *Robotics and Autonomous Systems*, 67(2015) 14-22.

29. Hart, P.E., Nilsson, N.J., and Raphael, B., A formal basis for the heuristic determination of minimum cost paths, *IEEE Transactions of Systems Science and Cybernetics*, 4(1968) 100-107.

30. Kopsov, I.E., and Sandvik, P.C., Analysis of subsea structure installation, paper presented at the *5th Int. Offshore and Polar Eng. Conf.*, Hague, the Netherlands, 1997.